water

MDPI

Article

Role of Ion Chemistry and Hydro-Geochemical Processes in Aquifer Salinization—A Case Study from a Semi-Arid Region of Haryana, India

Gopal Krishan [1,*], Priyanka Sejwal [1], Anjali Bhagwat [2], Gokul Prasad [1], Brijesh Kumar Yadav [3], Chander Prakash Kumar [1], Mitthan Lal Kansal [4], Surjeet Singh [1], Natarajan Sudarsan [1], Allen Bradley [5], Lalit Mohan Sharma [6] and Marian Muste [5]

1 Groundwater Hydrology Division, National Institute of Hydrology, Roorkee 247667, India; priyankasejwal6@gmail.com (P.S.); gokulghildiyal@gmail.com (G.P.); cpkumar@yahoo.com (C.P.K.); ssingh_sagar@yahoo.co.in (S.S.); sudarsan3010@gmail.com (N.S.)
2 Environmental Hydrology Division, National Institute of Hydrology, Roorkee 247667, India; anjali.civil.iit@gmail.com
3 Department of Hydrology, Indian Institute of Technology, Roorkee 247667, India; brijeshy@gmail.com
4 Department of Water Resources and Development Management, Indian Institute of Technology, Roorkee 247667, India; mlkgkfwt@iitr.ac.in
5 IIHR—Hydroscience & Engineering, the University of Iowa, Iowa City, IA 52242, USA; allen-bradley@uiowa.edu (A.B.); marian-muste@uiowa.edu (M.M.)
6 Sehgal Foundation, Gurgaon 122003, India; lalit.sharma@smsfoundation.org
* Correspondence: drgopal.krishan@gmail.com

Citation: Krishan, G.; Sejwal, P.; Bhagwat, A.; Prasad, G.; Yadav, B.K.; Kumar, C.P.; Kansal, M.L.; Singh, S.; Sudarsan, N.; Bradley, A.; et al. Role of Ion Chemistry and Hydro-Geochemical Processes in Aquifer Salinization—A Case Study from a Semi-Arid Region of Haryana, India. *Water* **2021**, *13*, 617. https://doi.org/10.3390/w13050617

Academic Editor: Helder I. Chaminé

Received: 17 December 2020
Accepted: 3 February 2021
Published: 26 February 2021

Abstract: In the present study, a total of sixty groundwater samples, twenty each for the pre-monsoon, monsoon and post monsoon seasons of 2018, were collected from selected locations in the Mewat district of Haryana, India. Electrical conductivity (EC) was measured at the site and total dissolved solids (TDS) were estimated. Samples were analysed for anions (chloride, sulphate, and bicarbonate) and cations (calcium, potassium, magnesium, and sodium). Multiple regression analysis was performed to analyse the data and report the dominant ions. Piper trilinear diagram and Gibbs plots were used to find out the water type and the factors controlling the chemistry of the groundwater, respectively. The saturation index of $CaCO_3$, $CaSO_4$ and NaCl was determined, using the PHREEQC MODEL. Sodium and calcium among cations, and chloride among the anions, had the highest degree of affinity and strong significance for all three seasons. The calcium–chloride water type dominated for all three seasons and Gibbs plot depicted that most of the $Na^+/Na^+ + Ca^{2+}$ and $Cl^-/Cl^- + HCO_3^-$ ratios show the weathering of rocks to form minerals as the major reason behind the ionic chemistry of the groundwater. The highest level of dissolution is encountered in the case of NaCl, followed by $CaSO_4$, whereas $CaCO_3$ depicts precipitation. The geochemical aspects of weathering, evaporation and ion exchange are the major processes responsible for high salinity, and anthropogenic activities are leading to its expansion. The findings from this study will be useful in management and remediation of groundwater salinity of the region.

Keywords: salinity; ions; semi-arid region; Mewat; Haryana

1. Introduction

The groundwater crisis in the northwest region of India is in the spotlight reported in recent studies [1–4]. Apart from decreasing groundwater levels [5,6], aquifer salinization has become a serious concern [7,8].

Salinization in water resources is associated with high concentrations of some chemical elements such as sodium, calcium, magnesium, sulphate, chloride, boron, fluoride, selenium, and arsenic [7]. Salinity is dynamically correlated with the local geological

factors and climatic conditions [9]. The various factors responsible for groundwater salinization are weathering, precipitation, ion exchanges, dissolution, leaching of fertilizers and manures and the subsurface biological activity. Since these processes depend upon the chemical and geological characteristics of Aquifer materials, the groundwater salinization varies both spatially and temporally [7,10,11]. Groundwater salinization is very rampant in state of Punjab and Haryana. Seven districts in the southwestern part of Haryana, namely Gurugram, Bhiwani, Rohtak, Kaithal, Mahindergarh, Mewat and Sonipat, cover approximately 30 percent of area of the state registers' saline groundwater [12].

Mewat, one of the 21 districts of Haryana, hovers on rain-fed agriculture due to the scanty irrigation sources. Despite unfavourable climatic conditions, agriculture is a significantly dominant contributor to livelihood. The growth and density of vegetation is relatively low due to the salinization of groundwater and limited amount of freshwater pockets; moreover, the TDS level of most of the locations reaches 35,000 mg/L [7]. Excessive amounts of specific dissolved ions outside their acceptance limits have detrimental effects on plant growth as well on the human health, which minimize agricultural production and reduce healthier practices. In order to address detrimental effects, it is vital to examine the associated hydro-geochemical process leading to the enhancement of salinity in groundwater as well as a need to maintain adequate planning, management and efficiency of groundwater resources. Keeping this in view, the present work aims to find the association between ion chemistry and hydro-geochemical processes in order to ascertain the role of ions in salinization of aquifer.

2. Study Area

2.1. Location and Climate

The research area is in Mewat district, Haryana, India, with a geographical extent of latitude 27° 39′, 28° 20′ N and longitude 76°51′, 77°20′ E (Figure 1). The study area covers about 1507 km^2 with a population of about one million [13]. The climate of the research area falls under semi-arid, with an annual rainfall of 594 mm with 75 percent received in monsoon season. In 2018, the annual rainfall in Nagina and Firozepur blocks was 650 and 724 mm, respectively, with more than 90 percent during June to September (Figure 2b). The daily maximum temperature of the study area is 40 °C (May and June) and daily minimum temperature is 5.1 °C (January). The recurrent shortage of rainfall during the monsoon season and limited availability of freshwater resources (Figure 2b) compel farmers to cultivate crops that require less water, such as wheat, millet and mustard.

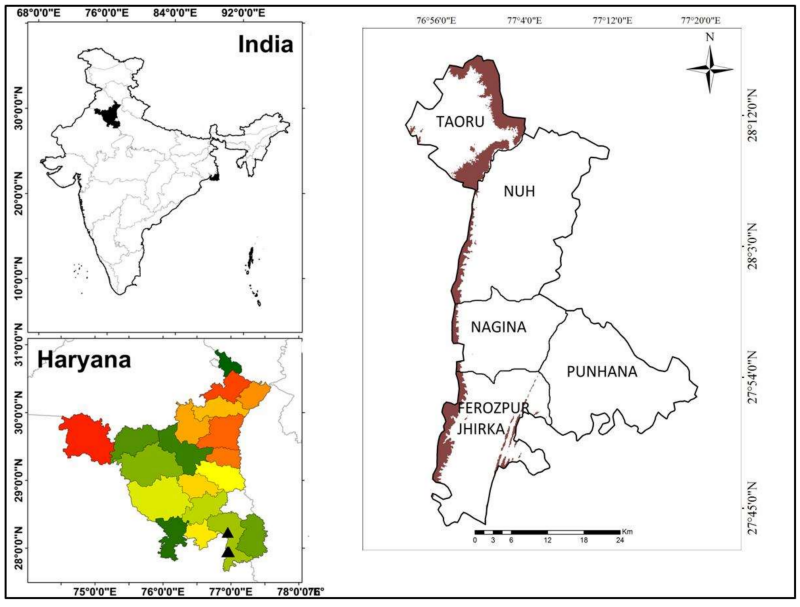

Figure 1. Location map of the study area depicting the district boundaries with Aravalli Hills.

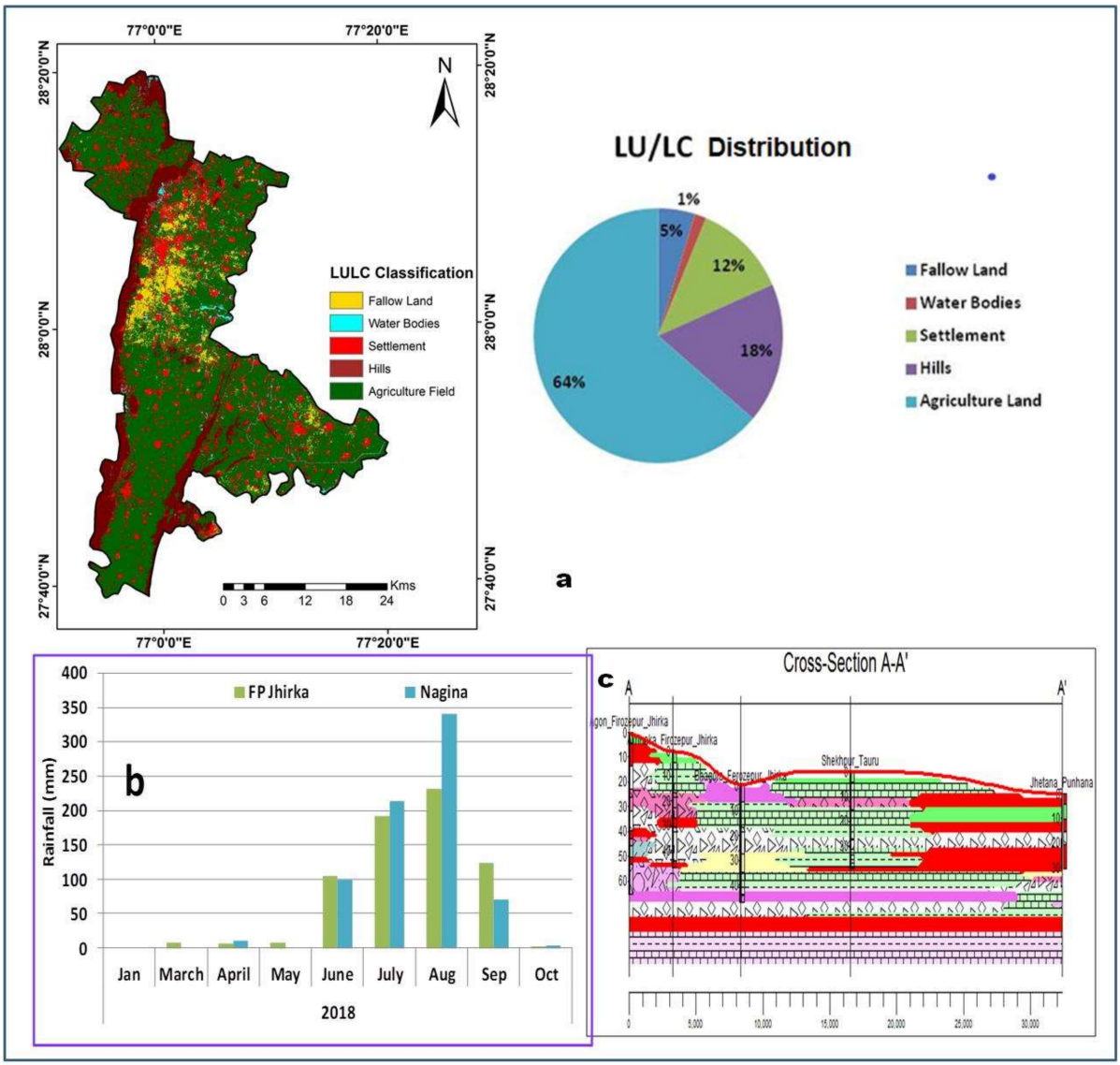

Figure 2. Landuse/land cover with class percentage distribution: (**a**) Landuse (**b**) rainfall; (**c**) lithology of study area.

2.2. Geomorphology and Soil

The district has a rolling topography with an urn-shaped structure. The central part is largely flat, but the western part slopes NW-SE and the northeastern parts slope NE-SW; altitude difference can be observed due to the presence of the Aravali Hills. The majority of the study area is dominated by the alluvial plains, with the northwestern area camouflaged by moderately deserted hills and valleys extending to the south-west and some parts of the south-east, whereas some parts of the mostly southeastern area are dominated by pediments and pediplain complexes with comparatively low water bodies.

Two major soil types, vertisols and salanchalks, are found in the study area. These soil types generally have medium textured loamy sand. The organic content of the soil ranges between 0.2 and 0.75 percent, while average electrical conductivity and the average pH of the soil are 0.80 µmhos/cm and 6.5–7, respectively. The top layer of the soil is significantly affected by salinization and salt crust can be found [14].

2.3. Hydrogeology

Topographically, the study area is mainly made up of alluvium of Quaternary and Paleoproterozoic age groups. The most dominant is the Quaternary age group alluvium, with a polycyclic sequence composed of sand, silt, and clay with kankar. The Paleoproterozoic age group consists of fledspathic gritty quartzite/amphibole/phyllite/schist of the Alwar group, Delhi (satellite data GSI). The groundwater has alluvial sediments with medium sand, clay and kankar. Good aquifer formations sand is intermittent, with multiple formations (Figure 2c). Overall, the clay ratio predominates at all depths throughout the districts. The depth of the bed rock in the central and eastern region lies within 300 mbgl, and the rest is around 90 mbgl in general [14]. The depth of water table ranges from 2 to 32 mbgl, with shallow water occurrences witnessed in the Nuh, Nagina and Punhana blocks.

2.4. Landuse and Land Cover

Agriculture is the main occupation of the people in the study area, as evident from landuse data, which consist of 64 percent agricultural land, 12 percent built-up area (human settlements including the residential sites), about 18 percent falls under hills, 1 percent under water bodies, and 5 percent under fallow area without perennial rivers and a normal semi-arid and arid drainage (Figure 2a). The major crops are Rabi, such as wheat, gram, and rice. The predominant economic activity includes agriculture, with no industrial settlement found in the area. Agriculture demands high irrigational water, but available water bodies do not meet these requirements. This creates a stress on the present water supplies in the study area.

3. Methodology

3.1. Sample Collection and Analysis

Groundwater samples from each of the 20 selected sites were collected in the pre-monsoon (April), monsoon (July), and post-monsoon seasons (October) in 2018 from hand pumps, open wells, and bore wells (Figure 3) with a depth range of 4–92 m. The water level of the open well in meters was recorded using a water-level indicator. GPS readings were taken to record latitude and longitude. Samples were taken in 125 mL capacity acid-washed Low-Density Polyethylene (LDPE) tarson bottles. Electrical Conductivity (EC) and pH were measured using a portable handheld Hach, HQ30d EC meter, and total dissolved solids (TDS) were estimated from measured EC values and expressed in mg/L. The samples collected in 125 mL bottles were analysed for cations (Ca^{2+}, Mg^{2+}, Na^{+}) and anions (HCO_3^{-}, SO_4^{2-}, Cl^{-}) at the water quality laboratory of the groundwater division of the institute, as per standard methodology [15].

The unpreserved 0.45µm filtered water samples were used for the analysis of cations (Ca^{2+}, Mg^{2+}, Na^{+}) and anions (HCO_3^{-}, SO_4^{2-}, Cl^{-}). Ca^{2+} and Mg^{2+} were determined titrimetrically using standard EDTA. Cl^{-} was determined by standard $AgNO_3$ titration method. HCO_3^{-} was determined by titration with HCl. Na^{+} was measured by flame photometry at a wavelength of 589 nm, and SO_4^{2-} by spectrophotometric turbidimetry by HACH spectrophotometer. All concentrations are expressed in milligrams per litre (mg/L).

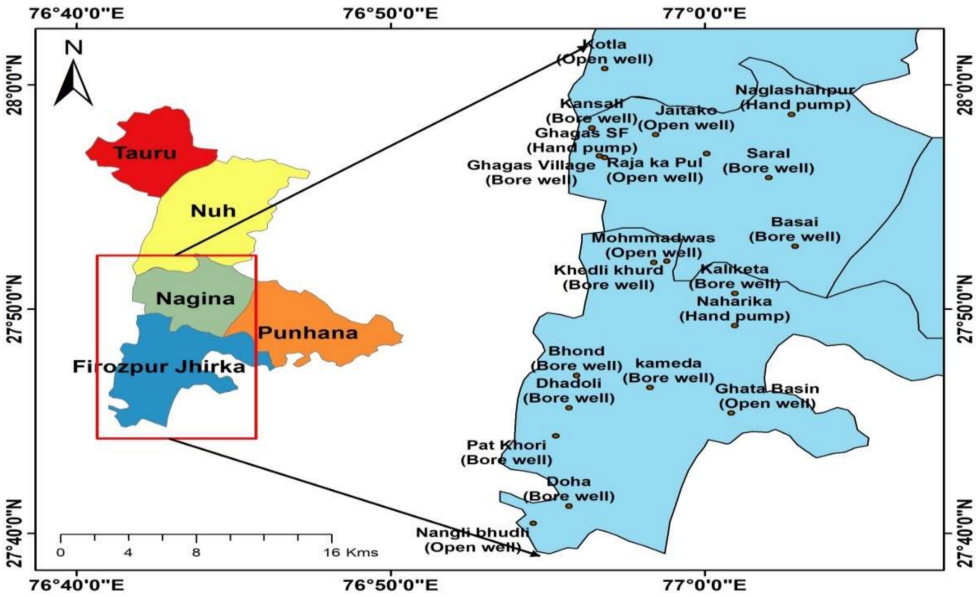

Figure 3. Sampling locations depicting sampled well type.

3.2. Data Analysis

Four trials were carried out in order to find the best-correlated value of TDS with respect to other ions. For all three seasons, the first trial included all six ions, namely Na^+, Cl^-, SO_4^{2-}, HCO_3^-, Mg^{2+} and Ca^{2+}. Regression Analysis was carried out using data analysis in Microsoft Excel to obtain the linear TDS equation and summative R^2 value. Multiple trails were performed and if the p-value did not satisfy the 95 percent level of significance, the respective ion was removed from the preceding trails.

AquaChem 2011.1 software was used to prepare piper trilinear diagram [16] in order to identify the hydro-geochemical facies and interpret the number of samples falling under the group sharing the same water qualities. Gibbs plots [17] was prepared using Sigma Plot 10 to interpret the factors controlling the ion chemistry of the groundwater. Arc GIS 10.4 was used for preparation of TDS maps using the inverse-distance weighting (IDW) interpolation technique.

4. Results and Discussion

Comparing all maps side-by-side shows that, in the southern part, the TDS in the pre-monsoon season is diluted in the monsoon season, which is evident from the increase in 0–1000 mg/L range values, which continues in the post-monsoon season with the withdrawal of rainfall. Similar observations were found using isotopes [18,19].

TDS level for all the seasons mostly lie in the 2000–12,000 mg/L range (Figure 4). Since TDS is a measure of all the dissolved salts that release cations and anions to water and has a direct relation with salinity, it is important to find out the dominant ion in the groundwater that elevates the level of salinity and its source.

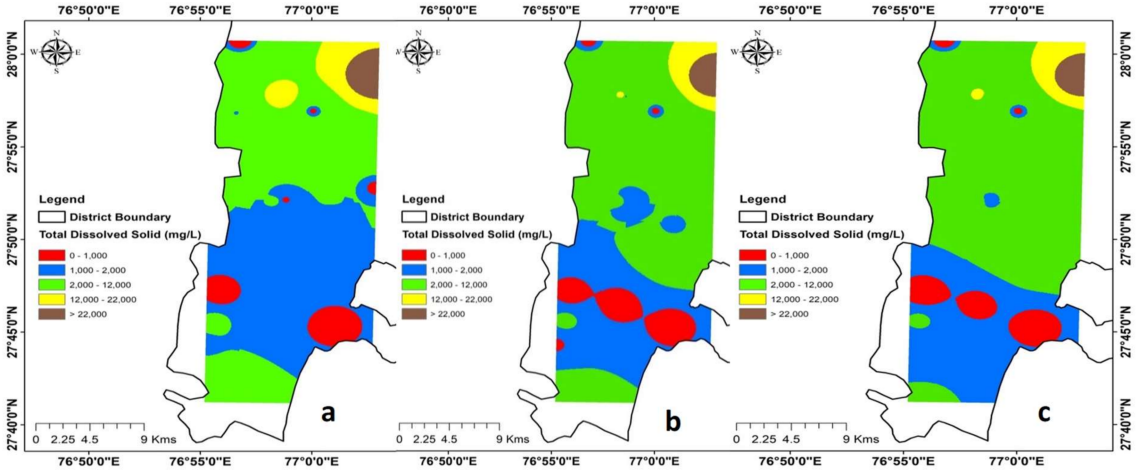

Figure 4. Total dissolved solids (TDS) maps (**a**) pre-monsoon (**b**) monsoon (**c**) post-monsoon.

4.1. Multiple Regression Analysis

In order to determine the dominant ions, multiple regression analysis was carried out. For all the seasons, three trails were carried out in accordance with the *p*-value with 95 percent significance level. The ions were removed if the value exceeded 0.05 and if all the ions fell under 95 percent significance level, then the one which had highest value relative to other ions was removed in the proceeding trail. Using this, two dominant cations and anions were determined. The dominant ions in the pre-monsoon were Cl^- and SO_4^{2-} from anions and Na^+ and Ca^{2+} from cations. The dominant ions in the monsoon season were Cl^- and HCO_3^- from anions, and Na^+ and Ca^{2+} from cations. The dominant ions in the post-monsoon season were Cl^- and SO_4^{2-} from anions and Na^+ and Mg^{2+} from cations. The compiled total of pre-monsoon and monsoon R^2 values was 0.99, and post-monsoon season value was 0.94 (Table 1).

Table 1. Different trails and dominant ion of each trail for all three seasons through Multiple Regression Analysis.

Parameters	Pre-Monsoon			Monsoon			Post-Monsoon		
	Trail	No. of Parameters	Dominant Ions	Trail	No. of Parameters	Dominant Ions	Trail	No. of Parameter	Dominant Ions
Na^+, Cl^-, Mg^{2+}, Ca^{2+}, SO_4^{2-}, HCO_3^-	1	6	Ca^{2+}, Na^+& Cl^-, SO_4^{2-}	1	6	Ca^{2+},Na^+& Cl^-,HCO_3^-	1	6	Mg^{2+},Na^+Cl^-, SO_4^{2-}
	2	5 (*Exc. Mg^{2+})	Ca^{2+}, Na^+& Cl^-, SO_4^{2-}	2	5 (*Exc. SO_4^{2-})	$Ca^{2+}Na^+$& Cl^-,HCO_3^-	2	5 (*Exc. HCO_3^-)	Mg^{2+},Na^+,Cl SO_4^{2-}
	3	4 (*Exc. HCO_3^- & Mg^{2+})	Ca^{2+},Na^+& Cl^-, SO_4^{2-}	3	4 (*Exc. SO_4^{2-} & Mg^{2+})	$Ca^{2+}Na^+$& Cl^-,HCO_3^-	3	4 (*Exc. HCO_3^- & Cl^-)	Mg^{2+},Na^+,Cl SO_4^{2-}
R^2		0.99			0.99			0.94	

*Exc.: excluding.

In order to understand the various processes responsible for the seasonal dominance of various ions, modeling of precipitation and dissolution process was carried out using PHREEQC model. SI was obtained for $CaCO_3$, $CaSO_4$ and NaCl from the model, as shown in (Table 2 and Figure 5). The highest level of dissolution was encountered in the case of NaCl, followed by $CaSO_4$, whereas $CaCO_3$ depicted precipitation. In pre-monsoon, SI for NaCl was −4.07 and for $CaSO_4$ was −1.38, which represents dissolution as a major reason for the dominance of Na^+ and Cl^- and Ca^{2+} and SO_4^{2-} ions.

Table 2. SI values of $CaCO_3$, $CaSO_4$ and NaCl using PHREEQC model.

Seasons	$CaCO_3$	$CaSO_4$	NaCl
Pre-monsoon	1.15	−1.38	−4.07
Monsoon	1.03	−0.99	−4.44
Post-monsoon	0.97	−0.88	−4.44

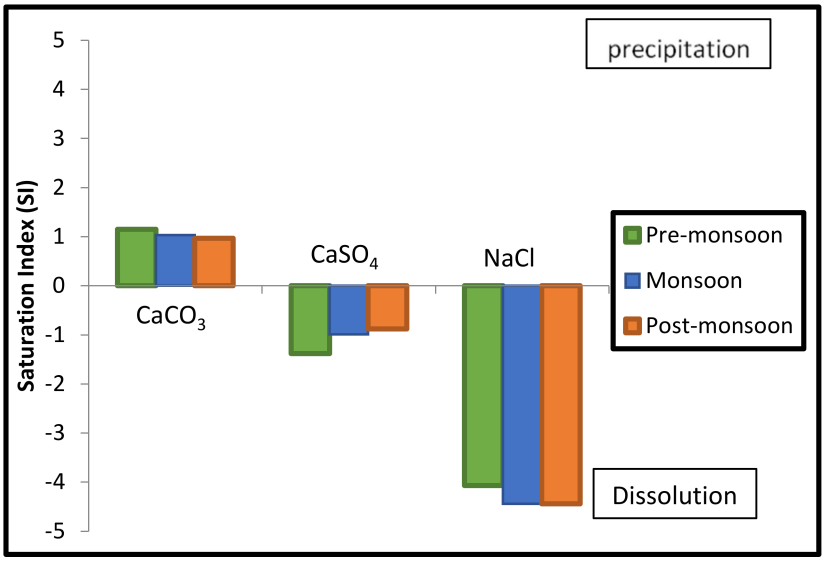

Figure 5. Season-wise trend of Saturation Index (SI) with respect to $CaCO_3$, $CaSO_4$ and NaCl in the groundwater of Mewat, Haryana, India.

In the monsoon season, SIs for NaCl and $CaSO_4$ are −4.44 and −0.99, which shows dissolution. Thus, Cl^-, Na^+, Ca^{2+} shows dominance; the SI for $CaSO_4$ reduced from −1.38 to -0.99 from the pre-monsoon to monsoon. HCO_3^- dissolution dominates over the SO_4^{2-} dissolution, making HCO_3^- dominant. This enhanced concentration is produced because, in case of monsoon season, the soil zone is the subsurface environment that contains elevated CO_2 pressure (produced as a result of the decay of organic matter and root respiration) which, in turn, combines with rainwater to form bicarbonate through the following reactions [20]:

$$CO_2 + H_2O \rightarrow H_2CO_3 \quad (1)$$

$$H_2CO_3 \rightarrow H^+ + HCO_3^- \quad (2)$$

Along with this, the monsoon rainfall results in the dissolution of carbonate and silicate minerals, as illustrated in Equation (3) [21]:

$$(\text{Cations})(\text{Silicates}) + H_2CO_3 \rightarrow H_4SiO_4 + HCO_3 + \text{cations} + \text{clay minerals} \quad (3)$$

In case of post-monsoon season Cl^-, Na^+, SO_4^{2-} becomes dominant as a result of the dissolution of NaCl and $CaSO_4$ with SI = −4.44 and −0.88, respectively. Apart from this Mg^{2+} becomes the dominant cation in this season; because of the common ion effect, the value of Ca^{2+} is suppressed as $CaCO_3$ (SI = 0.97) undergoes precipitation, and $CaSO_4$ (SI = −0.88) undergoes dissolution at the same time [22].

To understand the correlation between the different ions contributing to the TDS level and the ions present in the groundwater of the study area, the piper trilinear is drawn as shown in Figure 6, with its two triangles depicting anions on the right and cations on the left side. Six different delineations can be identified: 1—calcium chloride type; 2—magnesium bicarbonate type; 3—sodium bicarbonate type; 4—sodium chloride type; 5 and 6—mixed

type. The anion triangle on the right side illustrates that, for all three seasons, samples points fall in the H regions, which is the chloride dominant region, with some of the sample points shifting towards the mixed-type region E. However, for the cations in monsoon and post-monsoon seasons, approximately 50 percent of the sample points fall under the B region, that is, the Mg^{2+}-dominated region, and 50 percent of samples are distributed among the A, C and D regions with no clear delineation of any single cation's dominance. In the pre-monsoon season, 30 percent of the sample points fall under the B region, that is, the Mg^{2+}-dominated region, and the remaining 70 percent of samples are distributed among the A, C and D regions. In the diamond-shaped piper, for the pre-monsoon season, the dominant region was found to be the Ca^{2+} Cl^{-} type, with 55 percent of samples falling under this group, 25 percent of the samples falling under the mixed type and 20 percent under Na^{+} Cl^{-} type water. A similar pattern was seen in the case of monsoon season, with 85 percent of sample points falling under the Ca^{2+} Cl^{-} type water type and 15 percent of samples falling under the Na^{+} Cl^{-} type water. In the post-monsoon season, almost 90 percent of samples fall under the Ca^{2+} Cl^{-} type and only 10 percent under the Na^{+} Cl^{-} type water. In all three seasons, the dominant water type is Ca^{2+} Cl^{-}. This dominance of Ca^{2+} Cl^{-} type water can be explained by looking at the hydrogeology of the area. The aquifer study of Mewat has alluvial sediments, with medium sand, clay and kankar. The dissolution of $CaCO_3$ present in the soil is dissolved with the infiltration of rainwater and elevates Ca^{2+} and HCO_3^{-} ions concentration in groundwater.

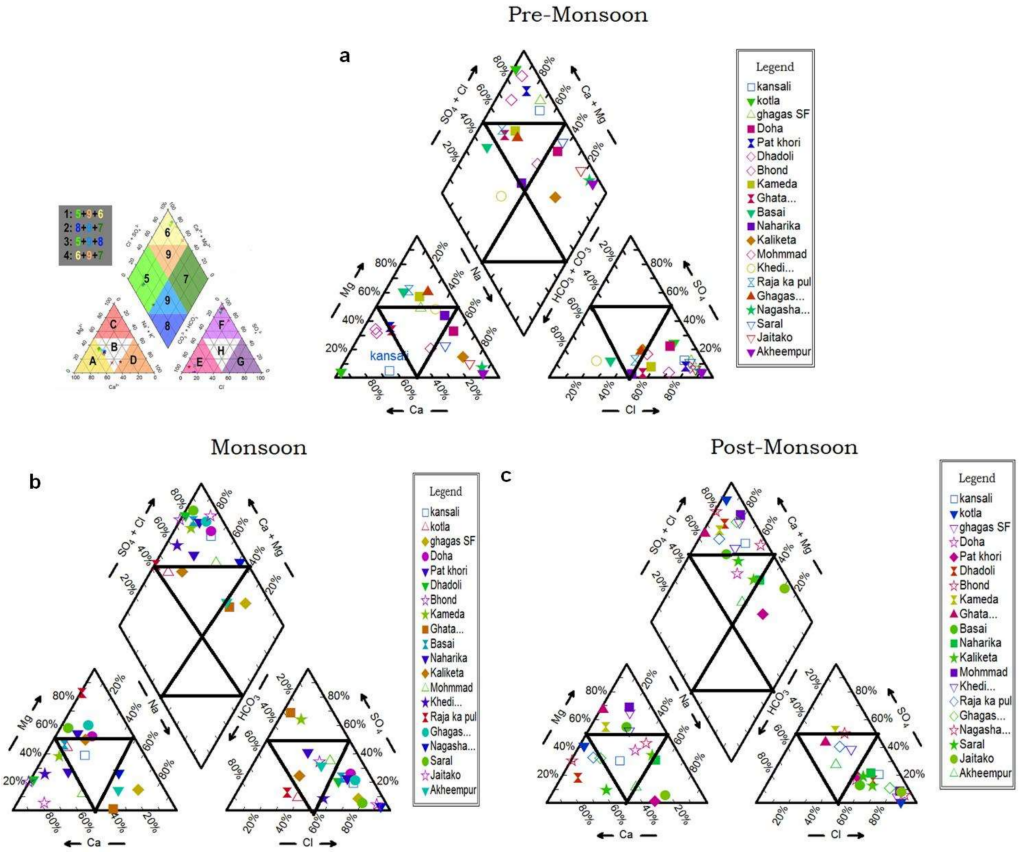

Figure 6. HREEQC modle. Piper trilinear diagram [16] of the groundwater water samples for (**a**) pre-monsoon (**b**) monsoon (**c**) post-monsoon. 1—calcium chloride type; 2—magnesium bicarbonate type; 3—sodium bicarbonate type; 4—sodium chloride type; 5 and 6—mixed type; A—mixed type; B—magnesium; C—sodium; D—calcium type, E—mixed, F—sulphate; G—bicarbonate; H—chloride.

The increase in ionic concentration of Ca^{2+} and HCO_3^- follows the groundwater level in the area, as shown in Figure 7. To justify the change in the ionic concentration with respect to the groundwater level, four different locations were taken randomly, and the ionic concentration was plotted against the groundwater level. As depicted in the graph, the groundwater level in the case of Mohmmadpur increased by 125 cm from pre-monsoon to post-monsoon and, as a result of increased groundwater level, the value of both Ca^{2+} (254 to 167 mg/L) and HCO_3^- (394 to 310) concentrations showed descending trends. Similarly, in the case of Bhond, the groundwater level increased by 25 cm from pre-monsoon to post-monsoon, and Ca^{2+} (176 to 167 mg/L) and HCO_3^- (165 to 84) concentrations showed a similar descending trend. However, in the case of Kotla, the reverse was noticed, i.e., the groundwater level showed a decreasing trend of 10 cm from pre- to post-monsoon, and the Ca^{2+} (138 to 1067) and HCO_3^- (34 to 365) concentrations showed an increasing trend. Therefore, as the groundwater level showed an increasing trend due to dissolution processes, the ionic concentration showed a decreasing trend and vice versa. Since the study area is dominated by agricultural practices, chloride in the groundwater is also contributed to by agricultural return flow, which also contributes to both the rise in groundwater level and the dissolution of ions contained in the soil [23,24].

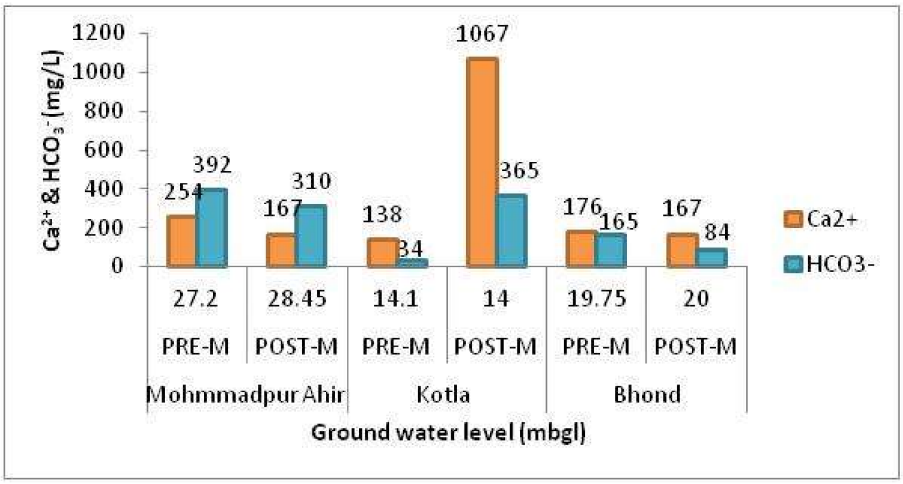

Figure 7. Seasonal change in Ca^{2+} and HCO_3^- ions with groundwater-level fluctuations.

4.2. Sources of Anions and Cations Causing Groundwater Salinization

The ion chemistry of the groundwater of the study area is described below to establish the correlation between the ions and the geochemical processes.

4.2.1. Weathering

To understand the dominance of cations and anions, plots are made between Ca^{2+} + Mg^{2+} and SO_4^{2-} + HCO_3^- (Figure 7). In the pre-monsoon and the monsoon, 20 percent of samples fall on the uniline and 80 percent fall below and near to the uniline. However, in the post-monsoon season, 25 percent of samples are lying on the uniline and 75 percent fall below and are not clustered near the uniline. As most of the sample points falls below the uniline (1:1), this depicts a higher concentration of Ca^{2+} and Mg^{2+} ions than that of SO_4^{2-} + HCO_3^-. In the pre-monsoon season, Ca^{2+} and Mg^{2+} ions lie in the range of 0–200 meq/L; in the monsoon, these range from 0 to 100 meq/L, and in the post-monsoon season, the range varies from 0 to 600 meq/L, making salinization more prominent in the post-monsoon season. The increased concentration of Ca^{2+} and Mg^{2+} ions can be attributed to rock (schist rock) and groundwater interaction, which is prominent in the hydrogeology

of the study area [25]. Apart from Schist, Amphibole dominants the Paleoproterozoic age group of rocks found in the study area. By the process of Hydrolysis, the Amphiboles are broken down, causing an increase in the concentration of Ca^{2+}, Mg^{2+}, Na^{+} ions [26]. Since the hydrogeology is dominated by fledspathic gritty quartzite, amphibole, phyllite and schist, it undergoes silicate weathering, making it one of the most prominent causes of enhanced concentrations of Mg^{2+} ions [27]. The enhanced concentration of Ca^{2+} and Mg^{2+} ions is further supported by the trilinear diagram (Figure 6), as it depicts calcium–chloride type water.

Na^{+} becomes the dominant ion in the pre- and post-monsoon seasons, as mentioned in Table 1. The increased concentration is contributed by the silicate weathering and the cation exchange process [21]. The cation exchange process takes places as shown in Equation (4)

$$Ca^{2+} + Na\text{-}X \rightarrow Ca\text{-}X + Na^{+} \quad (4)$$

where X denotes cation exchange sites.

When the infiltrating water interacts with clay lenses (fine-grained material that consists of hydrated aluminum silicate quartz, and organic fragments), the exchange between Ca^{2+} and Na^{+} ions is triggered.

4.2.2. Ion Exchange

The plots of $Ca^{2+} + Mg^{2+}$ versus $HCO_3^{-} + SO_4^{2-}$ (Figure 8a) are used to examine the role of ion exchange. Since most of the points fall below the uniline, this indicates a reverse ion exchange process [28]. In order to understand the ion exchange process taking place between the groundwater and aquifer material Choloro-Alkaline indices, CAI1 and CAI2 were calculated using Equations (5) and (6) [29,30]. The comparisons between both indices for the sampling sites in all the three seasons were plotted in Figure 8b.

$$CAI1 = [Cl^{-} - (Na^{+} + K^{+}]/Cl^{-} \quad (5)$$

$$CAI2 = [Cl^{-} - Na^{+} + K^{+}]/SO_4^{2-} + HCO_3^{-} + NO^{3-} \quad (6)$$

Figure 8b illustrates that in the pre-monsoon, 75 percent of samples have positive, and 25 percent of samples have negative values. However, in the monsoon and the post-monsoon seasons, 90 percent of samples show positive values and only 10 percent have negative values. The positive value indicates that the Base Exchange takes place between Na^{+} in the groundwater and Ca^{2+} or Mg^{2+} in the aquifer material. The negative value, on the other hand, indicates that ion exchange is taking place between Ca^{2+}–Mg^{2+} in the groundwater and Na^{+} in the aquifer material. Since the samples are dominated by positive values, reverse ion exchange explains the high concentration of Na^{+} in the groundwater.

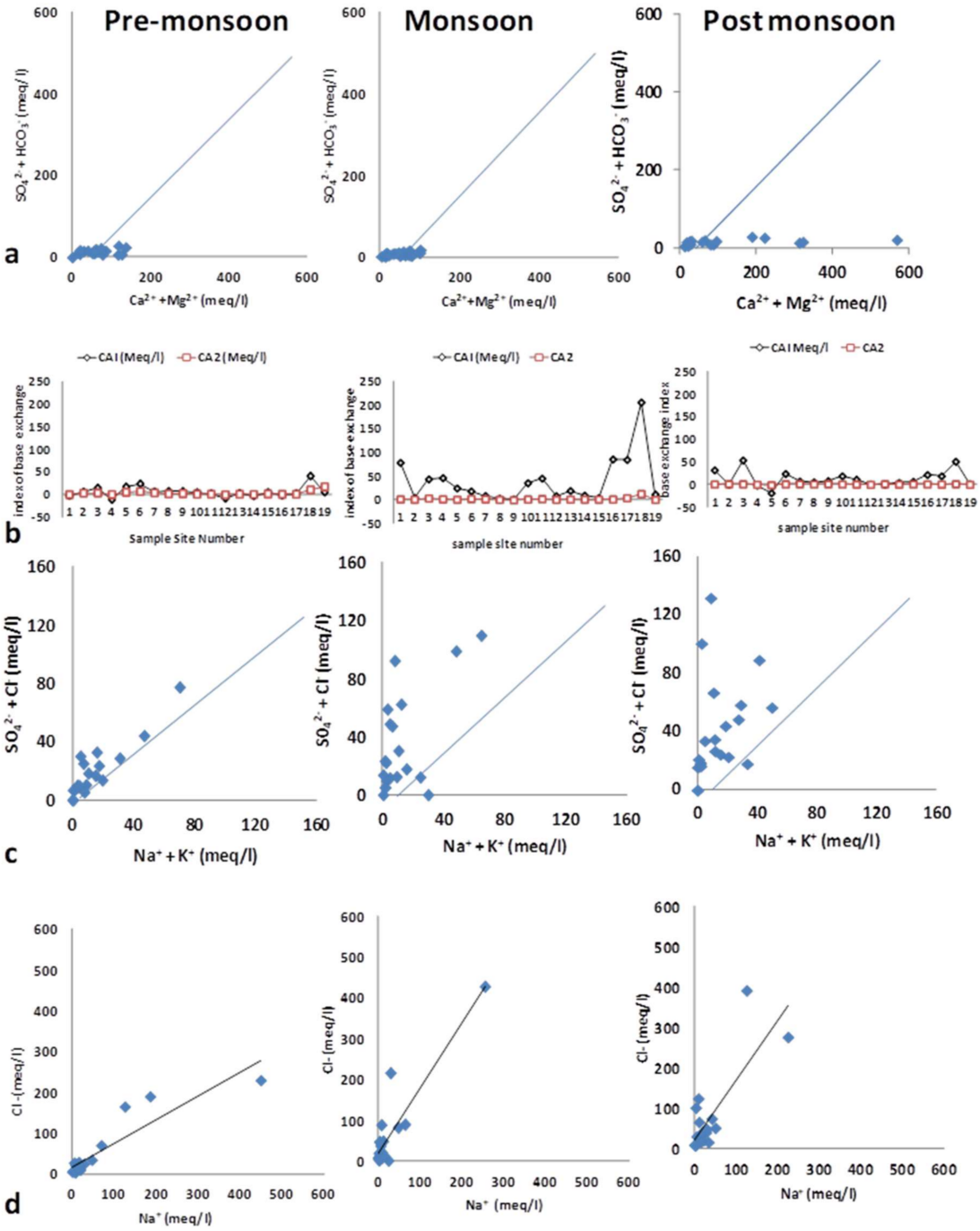

Figure 8. (**a**) Ca^{2+} +Mg^{2+} v/s SO_4^{2-}+ HCO_3^- (**b**) Base exchange indices (**c**) Na^++ K^+v/s SO_4^{2-}+ Cl^- (**d**) Na^+ v/s Cl^- for all 3 seasons.

4.2.3. Anthropogenic Sources

The results obtained from multiple linear regressions (Table 1) illustrate Cl^- as one of the dominant ions in the study area. These help to understand the sources responsible for the increase in the concentration of chloride, Na^+, K^+ v/s Cl^- + SO_4^{2-}, as shown in Figure 8c. In case of the pre-monsoon, 100 percent of sample points fall above the uniline. For the monsoon season, 90 percent fall above the uniline and 5 percent below the uniline, and 95 percent of sampling points are above the uniline and 5 percent below the uniline for the post-monsoon. Irrespective of season, the majority of sample plots above the uniline

indicate the dominance of Cl^{-} + SO_4^{2-}. The hydrogeology of the region is dominated by silicate minerals, but these silicate-bearing strata lack sodalite and chlorapatite minerals, which are known to be the sources of chloride and sulphate. Since no geological sources for chloride and sulphate are found in the region, anthropogenic sources dominated by agricultural activities can be thought as the major contributor of Cl^{-} and SO_4^{2-} ions [31].

The sulphate concentration is low in the pre-monsoon season, but the concentration increases in the monsoon season to the maximum in the post-monsoon season, as shown in Figure 8a–c. In the absence of any known geological reasons, the application of inorganic fertilizers such as potash (KCl) and gypsum ($CaSO_4 \cdot 2H_2O$) can be considered as the main sources of this increase [31]. The fertilizers are intensively applied for kharif crops during the monsoon and the post-monsoon period, which are also periods of maximum rainfall in Mewat; therefore, the leaching of minerals to groundwater becomes the main cause of sulphate contamination, which is also witnessed in the sulphate contour maps for the study area (Figure 9).

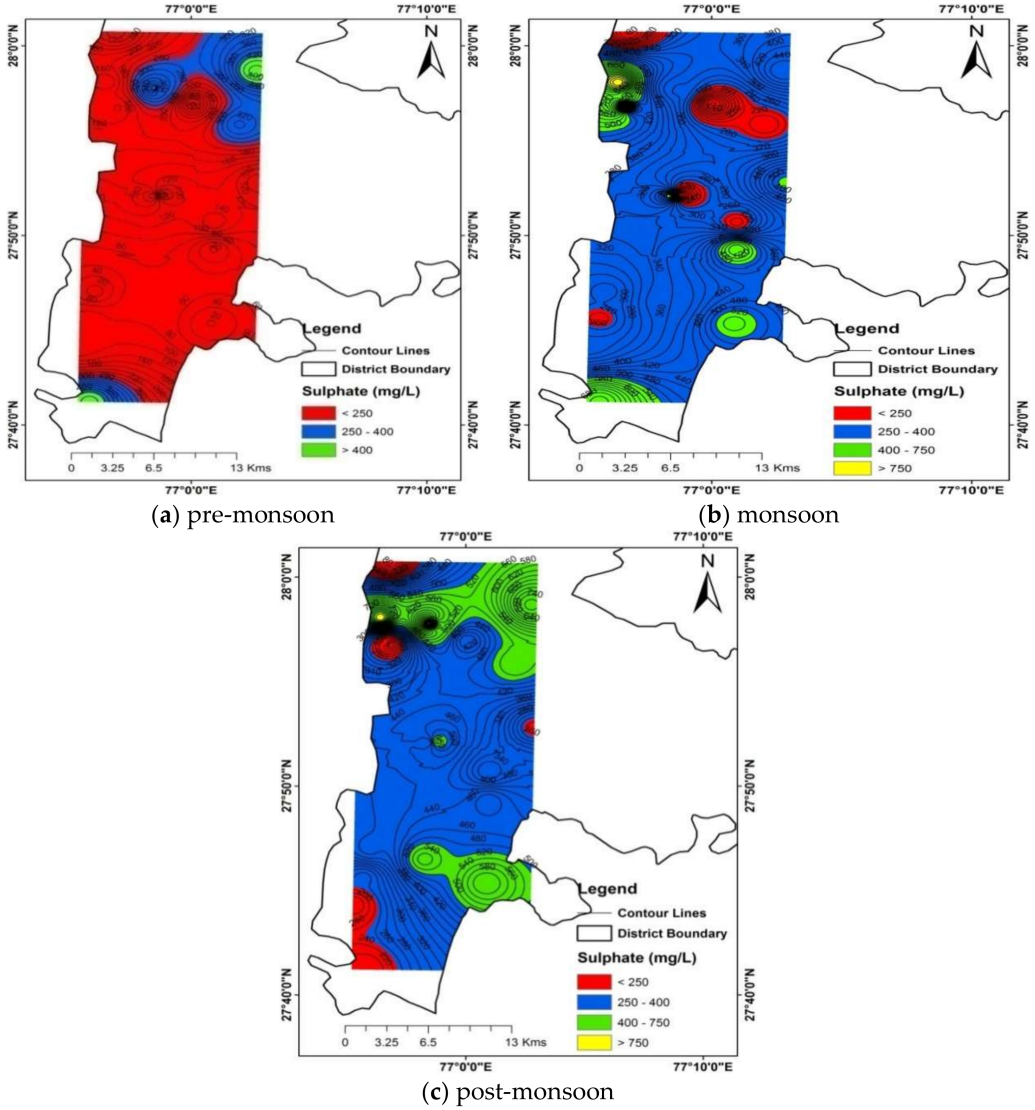

(**a**) pre-monsoon (**b**) monsoon

(**c**) post-monsoon

Figure 9. Contour map of sulphate for (**a**) pre-monsoon (**b**) monsoon (**c**) post-monsoon.

4.2.4. Evaporation

Na^+ v/s Cl^- plots (Figure 8d) show that the points falling near to the uniline (1:1) are considerable, due to the process of evaporation. The Quaternary age group of the study area is dominated by sand, silt, and clay with kankar ($CaCO_3$), which reinforce the vigorous acquaintance of evaporation in the study area and are elevated by the presence of a semi-arid climate [21,32]. The sample points fall above the uniline in all three seasons, depicting the higher concentrations of chloride ion. The above-mentioned reasons, along with the natural geography, Aravalli ranges and rise in temperature, play a major role in groundwater salinity.

Gibbs plots illustrate (Figure 10) the factors influencing the ion chemistry, i.e., rock, precipitation and evaporation dominance. The plot shows the chemical weathering of rocks to form minerals as the major reason governing the groundwater chemistry in the study area. Higher anthropogenic activities increase the concentration of TDS which, in turn, shifts some of the sample points from rock- to evaporation-dominant regions [33] Similar results are found for semi-arid areas [34–36] where, through tracer techniques, it has been observed that the mineral dissolution is major cause of salinity.

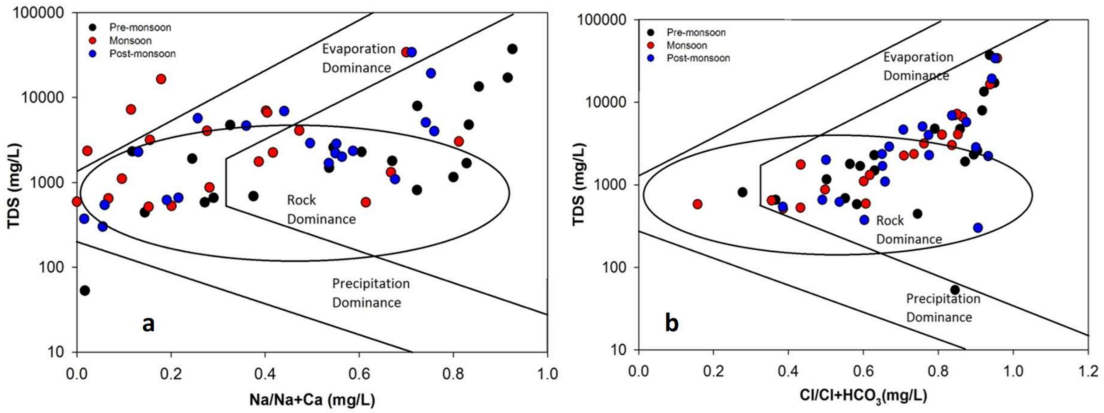

Figure 10. Gibbs plots (**a**) TDS v/s $Na^+/Na^+ + Ca^{2+}$ and (**b**) TDS v/s $Cl^-/Cl^- + HCO_3^-$.

5. Conclusions

In the semi-arid Mewat region of Haryana, where more than half of groundwater samples that were collected in 2018 for pre-monsoon, monsoon, and post-monsoon seasons were categorized as saline water, this study has led to an understanding of the region in terms of its high groundwater salinity. The salinity is caused due to the dominance of Na^+, Cl^- and Ca^{2+} ions, and these ions have a strong positive correlation with TDS. The processes responsible for the dominance of these ions are weathering, evaporation and ion exchange. The primary source of salinity in the study area is found to be geogenic, further enhanced by anthropogenic activities. These results will be useful in the management of groundwater salinity and planning for remediation measures in the region. The Aquifer Storage and Recovery (ASR) technique for storage of fresh water in saline water has been tested under controlled conditions and will now be transferred to field conditions at a large scale.

Author Contributions: Conceptualization, methodology, funding acquisition, review and editing: G.K.; Writing, original draft preparation: P.S.; writing—review and editing: A.B. (Anjali Bhagwat); Formal analysis: G.P.; Data curation: B.K.Y.; project administration: C.P.K.; visualization: M.L.K.; validation: S.S.; software: N.S.; review and editing: A.B. (Allen Bradley); investigation: L.M.S.; supervision: M.M. All authors have read and agreed to the published version of the manuscript.

Funding: This work was carried out under Purpose Driven Study under National Hydrology Project funded by World Bank.

Institutional Review Board Statement: Not applicable.

Informed Consent Statement: Not applicable.

Data Availability Statement: Available on request from corresponding author.

Acknowledgments: GK thanks Director, National Institute of Hydrology, Head, GWHD, Nodal officer, NHP, PDS Coordinator, NHP training coordinator, NPMU-NHP, TAMC, Funding received from National Hydrology Project is duly acknowledged.

Conflicts of Interest: The authors declare that they have no conflict of interest.

References

1. Bonsor, H.C.; MacDonald, A.M.; Ahmed, K.M.; Burgess, W.G.; Basharat, M.; Calow, R.C.; Dixit, A.; Foster, S.S.D.; Gopal, K.; Lapworth, D.; et al. Hydrogeological typologies of the Indo-Gangetic basin alluvial aquifer, South Asia. *Hydrogeol. J.* **2017**, *25*, 1377–1406. [CrossRef]
2. Krishan, G.; Bisht, M.; Ghosh, N.C.; Prasad, G. Groundwater salinity in north west of India: A critical appraisal. In *Environment Management*; WSTL Book Series; Springer: Berlin/Heidelberg, Germany, 2019; Chapter 19.
3. Lapworth, D.J.; MacDonald, A.M.; Krishan, G.; Rao, M.S.; Gooddy, D.C.; Darling, W.G. Groundwater recharge and age-depth profiles of intensively exploited groundwater resources in northwest India. *Geophys. Res. Lett.* **2015**, *42*. [CrossRef]
4. MacDonald, A.; Bonsor, H.; Ahmed, K.; Burgess, W.; Basharat, M.; Calow, R.; Dixit, A.; Foster, S.; Krishan, G.; Lapworth, D.; et al. Groundwater depletion and quality in the Indo-Gangetic Basin mapped from in situ observations. *Nat. Geosci.* **2016**, *9*, 762–766. [CrossRef]
5. Malik, A.; Bhagwat, A. Modelling groundwater level fluctuations in urban areas using artificial neural network. *Groundw. Sustain. Dev.* **2021**, *12*, 100484. [CrossRef]
6. Rodell, M.; Velicogna, I.; Famiglietti, J.S. Satellitebased estimates of groundwater depletion in India. *Nature* 2009. [CrossRef]
7. Krishan, G. Groundwater Salinity. *Curr. World Environ.* **2019**, *14*, 186–188. [CrossRef]
8. Lapworth, D.; Krishnan, G.; Macdonald, A.; Rao, M. Groundwater quality in the alluvial aquifer system of northwest India: New evidence of the extent of anthropogenic and geogenic contamination. *Sci. Total Environ.* **2017**, *599–600*, 1433–1444. [CrossRef] [PubMed]
9. Misra, A.K.; Mishra, A. Study of quaternary aquifer in Ganga Plains, India: Focus on groundwater salinity, fluoride and fluorosis. *J. Hazard. Mater.* **2006**, *144*, 438–448. [CrossRef]
10. Pazand, K.; Ardeshir, H. Investigation of hydrochemical characteristics of groundwater in the Bukan basin, North. *Iran. Appl. Water Sci.* **2012**, *2*, 309–315. [CrossRef]
11. Lakshmanan, A.R.; Kannan, M.; Senthil, K. Major ion chemistry and identification of hydrogeochemical processes of groundwater in a part of Kancheepuram district, Tamil Nadu, India. *Environ. Geosci.* **2003**, *10*, 157–166. [CrossRef]
12. Anjali, P.; Saravanan, V.S.; Jayanti, C. *Interlacing Water and Human Health: Case Studies from South Asia*; SAGE Publishing Pvt. Ltd.: Thousand Oaks, CA, USA, 2012; pp. 201–207.
13. CENSUS. 2011. Available online: http://www.census2011.co.in/census/district/226-mewat.html (accessed on 1 August 2020).
14. Central Ground Water Board. Ground Water Information Booklet, Mewat District, Haryana. 2012. Available online: www.cgwb.gov.in/district_profile/haryana/mewat.pdf (accessed on 1 August 2020).
15. APHA. *Standard Methods for The Examination of Water and Wastewater*, 21st ed.; American Public Health Association: Washington, DC, USA; New York, NY, USA, 2005.
16. Piper, A.M. A graphical procedure in the geochemical interpretation of water analysis. *Eos Trans. Am. Geophys. Union* **1944**, *25*, 914–928. [CrossRef]
17. Gibbs, R.J. Mechanisms Controlling World Water Chemistry. *Science* **1970**, *170*, 1088–1090. [CrossRef]
18. Krishan, G.; Ghosh, N.C.; Kumar, C.P.; Sharma, L.M.; Yadav, B.; Kansal, M.L.; Singh, S.; Verma, S.K.; Prasad, G. Understanding stable isotope systematics of salinity affected groundwater in Mewat, Haryana, India. *J. Earth Syst. Sci.* **2020**, *129*, 109. [CrossRef]
19. Krishan, G.; Kumar, C.P.; Prasad, G.; Kansal, M.L.; Yadav, B.; Verma, S.K. Stable Isotopes and Inland Salinity Evidences for Mixing and Exchange. In Proceedings of the Roorkee Water Conclave (RWC-2020), Uttarakhand, India, 26–28 February 2020.
20. Singh, A.K.; Mondal, G.C.; Kumar, S.; Singh, T.B.; Tewary, B.K.; Sinha, A. Major ion chemistry, weathering processes and water quality assessment in upper catchment of Damodar River basin, India. *Environ. Geol.* **2007**, *54*, 745–758. [CrossRef]
21. Subba Rao, N.; Surya Rao, P. Major ion chemistry of groundwater in a River basin: A study of India. *Environ. Earth Sci.* 2009. [CrossRef]
22. Freeze, R.A.; Cherry, J.A. *Groundwater*; Presentice Hall: Upper Saddle River, NJ, USA, 1979.
23. Hem, J.D. *Study and Interpretation of the Chemical Characteristics of Natural Water*; Scientific Publisher: Jodhpur, India, 1991; p. 2254.
24. Todd, D.K. *Groundwater Hydrology*, 2nd ed.; John Wiley: New York, NY, USA; Chichester, UK; Brisbane, Australia; Toronto, ON, Canada, 1980; Volume xiii, p. 535.
25. Craw, D. Water-rock interaction and acid neutralization in a large schist debris dam, Otago, New Zealand. *Chem. Geol.* **2000**, *171*, 17–32. [CrossRef]

26. Malov, A.I. Water–rock interaction in vendian sandy–clayey rocks of the Mezen Syneclise. *Lithol. Miner. Res.* **2004**, *39*, 345–356. [CrossRef]
27. Holland, H.D. *The Chemistry of the Atmosphere and Ocean*; Wiley—Intersciences: New York, NY, USA, 1978; p. 351.
28. Fisher, R.S.; Mullican, W.F. Hydrochemical evolution of sodium sulphate and sodium-chloride groundwater beneath the Northern Chihuahuan desert, Trans-Pecos, Texas, USA. *Hydrogeol J.* **1997**, *5*, 4–16. [CrossRef]
29. Schoeller, H. Qualitative evaluation of groundwater resources. In *Methods and Techniques of Groundwater Investigations and Development*; UNESCO Water Resources Series 33; UNESCO: Paris, France, 1965; pp. 44–52.
30. Schoeller, H. Geochemistry of groundwater. In *Groundwater Studies—An International Guide for Research and Practice*; UNESCO: Paris, France, 1977; Chapter 15; pp. 1–18.
31. Rajmohan, N.; Elango, L. Hyrogeochemistry and its relation to groundwater level fluctuation in the Palar and Cheyyar River basins, southern India. *Hydrol. Process* **2006**, *20*, 2415–2427. [CrossRef]
32. Gurdak, J.J.; Hanson, R.T.; McMohan, P.B.; Bruce, B.W.; McCray, J.E.; Thyne, G.D.; Reedy, R.C. Climate variability controls on unsaturated water and chemical movement, High Plans Aquifer, USA. *Vadose Zone J.* **2007**, *6*, 533–547. [CrossRef]
33. Subba Rao, N. Groundwater quality in crystalline terrain of Guntur district, Andhra Pradesh. *Visakhapatnam J. Sci.* **1998**, *2*, 51–54.
34. Krishan, G.; Prasad, G.; Anjali; Kumar, C.; Patidar, N.; Yadav, B.; Kansal, M.; Singh, S.; Sharma, L.; Bradley, A.; et al. Identifying the seasonal variability in source of groundwater salinization using deuterium excess- A case study from Mewat, Haryana, India. *J. Hydrol. Reg. Stud.* **2020**, *31*, 100724. [CrossRef]
35. Krishan, G.; Vashisth, R.; Sudersan, N.; Rao, M.S. Groundwater salinity and isotope characterization: A case study from south-west Punjab, India. *Environ. Earth Sci.* **2021**, (in press).
36. Krishan, G.; Ghosh, N.C.; Kumar, B.; Kumar, C.P.; Rao, M.S.; Sudarsan, N.; Singh, S.; Sharma, A.; Kumar, S.; Jain, S.K. *Aquifer Salinization in Punjab*; Report-CS-175/GWHD/2019-20 Submitted to PSFC; Government of Punjab: Chandigarh, India, 2021; p. 178.